

# Determination of Water Distribution and Mobility Inside Maize Kernels During Steeping Using Magnetic Resonance Imaging

RONGSHENG RUAN and J. BRUCE LITCHFIELD<sup>1</sup>

## ABSTRACT

Cereal Chem. 69(1):13-17

Differences in water content and mobility in various components of corn kernels during steeping were measured by magnetic resonance imaging. The proton density and  $T_1$  images (water distribution and mobility mapping) were obtained with a spatial resolution of 100  $\mu\text{m}$ . The outside steepwater signal was well suppressed and the inside structure

of the corn kernel was revealed clearly with proton density ( $\rho$ ), spin-lattice relaxation ( $T_1$ ), and apparent spin-spin relaxation ( $T_2^*$ ) images. The technique enabled clear definition of the principal tissues in corn kernels and provided quantitative information concerning differences in water distribution and mobility.

Corn is the most important cereal crop in the United States, where annual corn production is more than double that of any other crop. Approximately 15% of the annual U.S. corn production is processed by wet milling to produce starch as a final product or starch for subsequent conversion into sweeteners and ethanol. The steeping operation is a critical step in corn wet milling processes. Present steeping technology has existed for over 100 years, and many things, such as reducing steeping time, could be done to improve the current process and reduce the cost. However, to do this, it is important to obtain some fundamental information such as the water distribution and mobility inside the corn kernel during steeping.

Magnetic resonance imaging (MRI) is a technique for producing images of heterogeneous systems based on the nuclear magnetic resonance (NMR) properties of a bulk fraction distributed within the sample (Morris, 1986). In most food materials, the largest fraction is likely to be the water, although, in some imaging pulse sequences, lipids may need to be taken into account due to the chemical shift effect. Frequently used NMR properties include the proton spin density ( $\rho$ ), spin-lattice relaxation time ( $T_1$ ), spin-spin relaxation time ( $T_2$ ), and the diffusion coefficient ( $D$ ). The  $\rho$  directly reflects the apparent water content, whereas  $T_1$  is inversely correlated with the fraction of bound water, or water that is hydrogen-bound to larger macromolecules for a period comparable to  $T_1$  (Johnson et al 1987). In other words,  $T_1$  is correlated with water mobility.

The study of water in foods, in fact, was a very early application of NMR; however, the use of MRI to study foods is still in its infancy. MRI technology has great potential as a tool for the study of foods, as it is noninvasive and nondestructive and gives high accuracy and high resolution.

Currently, the most frequently used MRI technique is the Hahn spin-echo technique, in which the signal intensity ( $S$ ) of each voxel is (Stark and Bradley, 1988):

$$S = \rho [1 - 2e^{-TR-(TE/2)} + e^{-TR/T_1}] e^{-TE/T_2} e^{-bD} \quad (1)$$

TR is the repetition delay time between successive pulse sequences; TE is the time between the excitation radio frequency (rf) pulse and the echo formation pulse; and  $b$  is the diffusion factor. For example, Jenner et al (1988) used this technique to study the circulation of water within high-moisture wheat grains. Song and Litchfield (1990) used it to study the drying of corn. Ruan et al (1989) studied the drying and water absorption of potatoes with this technique, and Chen et al (1989) evaluated the internal quality of fruits and vegetables with it.

However, corn steeping involves a solid-liquid diffusion system,

in which the corn kernel has a relatively lower proton concentration whereas the steepwater generates a large signal, which causes dynamic range problems (Wehrli et al 1983). Moreover, corn kernels have a very short  $T_2$  of about 4 msec. Therefore, it is difficult to obtain a clear image of the corn kernel with the conventional spin-echo technique.

Fortunately, the  $T_1$  of the corn kernel is also much shorter than that of the steepwater. In other words, steepwater requires a much longer time than a corn kernel for signal recovery. Therefore, short intrapulse sequence delay time (TR) may be used together with the small flip angle technique (that is, using less than a 90° rf excitation pulse) so that only signals from the corn kernel can be effectively recovered and the steepwater signal can be saturated and suppressed.

The gradient-refocused echo technique, or fast low-angle shot (FLASH), uses readout gradient reversals for magnetization refocusing instead of adding the 180° rephasing pulse, as in the Hahn spin-echo technique. This way, the time between the excitation rf pulse and the echo formation depends mainly on the rate at which the gradient rises and falls and can be greatly reduced, so that the  $T_2$  decay and the diffusion signal loss can be decreased. The gradient echo technique also makes the small flip angle excitations more efficient. Therefore, this technique may be used to study the steeping of the corn kernel.

The  $S$  resulting from the gradient echo imaging technique depends on three independent parameters: TR, the echo delay time (TE), and the small flip angle ( $\theta$ ) (Stark and Bradley 1988). The  $S$  of each voxel is (Stark and Bradley 1988):

$$S = \rho \frac{(1 - e^{-TR/T_1}) \sin \theta}{1 - e^{-TR/T_1} e^{-TR/T_2} (e^{-TR/T_1} - e^{-TR/T_2}) \cos \theta} e^{-TE/T_2^*} \quad (2)$$

$T_2^*$  is used in the term  $\exp(-TE/T_2^*)$  instead of  $T_2$  because the transverse relaxation during the TE occurs not only due to  $T_2$  effects (spin-spin interactions), but also due to the magnetic field inhomogeneities and magnetic susceptibility inhomogeneities, which are not eliminated by the reversal of the readout gradient. In the case of corn kernels,  $T_2$  is very small, so the signal expression can be simplified to:

$$S = \rho \frac{(1 - e^{-TR/T_1}) \sin \theta}{(1 - e^{-TR/T_1} \cos \theta)} e^{-TE/T_2^*} \quad (3)$$

Equation 3 indicates that the  $T_1$  image, or the water mobility mapping, can be obtained by 1) keeping TE and  $\theta$  constant, 2) acquiring images with a series of values of TR, and 3) performing a nonlinear regression fitting. The  $T_2^*$  image can be obtained by 1) keeping TR and  $\theta$  constant, 2) acquiring images with a series of TE settings, and 3) performing the linear regression fitting. Therefore, in either  $T_1$ -weighted images or  $T_2^*$ -weighted images,  $\rho$  is the only unknown in equation 3 for each voxel. Then, the  $T_1$  and  $T_2^*$  effects can be eliminated, so that the proton density image, or the water distribution mapping, can also be obtained.

<sup>1</sup>Graduate assistant and assistant professor, respectively, Agricultural Engineering Department, University of Illinois, Urbana 61801.

Mention of product or trade name does not imply any endorsement by the University of Illinois.

The objective of this study was to develop a method for investigating the water mobility and distribution inside the corn kernel during steeping.

## MATERIALS AND METHODS

A spectroscopy imaging system with a 200-MHz, 4.7-tesla, 330-mm bore diameter instrument and a microscopic imaging probe (Doty Scientific, Inc., Columbia, SC) were used for the MRI data acquisition. The rf coil region of the probe was 17 mm (longitudinal direction), and the clear bore of the probe was 12 mm. The probe permits acquisition of high-resolution imaging data because of its small rf receiver coils, high and linear magnetic field gradients, and fast pulse and signal response time.

Since this was a study to develop the MRI technique, the steeping experiments were done at room temperature, with no lactic acid or  $\text{SO}_2$  added to the steepwater. To ensure a strong signal, the initial moisture content of the corn kernels was about 35% (wb). The kernel was steeped in an NMR test tube (11-mm i.d.), and was held in place by a small rubber ring (Fig. 1).

Since corn kernels are complex in structure and composition, both  $T_1$  and  $T_2$  differ with position. Therefore, both theoretical calculation of the best  $\theta$  and actual acquisition of the images with different parameter settings were performed to select the TR and  $\theta$  settings for the  $T_1$ -weighted images. The theoretical calculation of the best  $\theta$  was based on the average  $T_1$  of each of the principle components, germ and endosperm, and the best short TR. TRs of 0.05, 0.10, 0.15, and 0.20 sec were set with a constant small flip angle of  $45^\circ$  and a constant TE of 0.0042 sec for the acquisition of four  $T_1$ -weighted images. Similarly, four TEs were selected (0.0028, 0.0042, 0.0056, and 0.007 sec) based on the best possible short TE and the actual acquired images. The constant intrapulse TR was set to 0.10 sec and the constant small flip angle to  $45^\circ$  for the four  $T_2^*$ -weighted images. A summary of the parameter settings for the MRI data acquisition is shown in Table I.

The three-dimensional (3D) FLASH sequence was used for the MRI data acquisition. Although a two-dimensional (2D)

imaging sequence takes less time to obtain an image, it requires the long-slice selective pulses for the 2D imaging, which makes the short echo time TE impossible. As a result, 2D imaging sequences were not suitable for samples with a short  $T_2$ , such as corn kernels. The field of view for the 3D FLASH sequence was set to 1.3 cm in each direction. The linear magnetic field gradients used were about 0.6 millitesla per centimeter, or 6 gauss per centimeter. Two sets of data, a total of 16 3D ( $128 \times 128 \times 64$ ) images, were acquired. Each set of images, including four  $T_1$ -weighted and four  $T_2^*$ -weighted images, took about 2.5 hr to acquire.

The MRI data acquired from the imaging system were processed and reconstructed with image processing software (Viewit 1990). A nonlinear regression program, which transforms the nonlinear equation into linear operation, was written to fit the  $T_1$ -weighted image data with equation 3 for the  $T_1$  mapping. A linear regression program for the  $T_2^*$  data fitting and the proton density image data calculation program were also developed. Since all the data sets were relatively large, a Cray-2 supercomputer was used for the calculations.

## RESULTS AND DISCUSSION

One of the 3D images of a corn kernel during steeping was reconstructed (Fig. 2). Forty 2D ( $128 \times 128$ ) sequential slices of the 3D image, from slice number 16 to slice number 55, are shown in Figure 3. The spatial resolution of the 2D slices was about  $100 \mu\text{m}$ . The corn kernel can be seen clearly, which indicates that the signal from the water surrounding the corn kernel was well saturated and suppressed by this imaging technique.

A slice of the corn kernel in each of the four  $T_1$ -weighted images is shown in Figure 4, where the signal intensity increased as TR increased. The time required to acquire each 3D image data also increased with the increase of the TR value. The same slice of the corn kernel in each of the four  $T_2^*$ -weighted images is shown in Figure 5, where the signal intensity decreased with increased TE, or the transverse magnetization decay time before the echo formation. These all agreed with equation 3.

Two  $T_2^*$  mappings were obtained from the linear regression

TABLE I  
Summary of Parameter Settings for Magnetic Resonance Imaging Data Acquisition

Image <sup>a</sup>	Repetition Delay Time (sec)	Echo Delay Time (msec)	Field of View	Gradient <sup>b</sup> (mT/cm)	Flip Angle (degree)
$T_1$ -weighted	0.05; 0.10; 0.15; 0.20	4.2	(1.3 cm) <sup>3</sup>	0.6	45
$T_2^*$ -weighted	0.10	2.8; 4.2; 5.6; 7.0	with $128 \times 128 \times 64$		

<sup>a</sup> $T_1$  = spin-lattice relaxation time;  $T_2^*$  = spin-spin relaxation time.

<sup>b</sup>mT = millitesla.

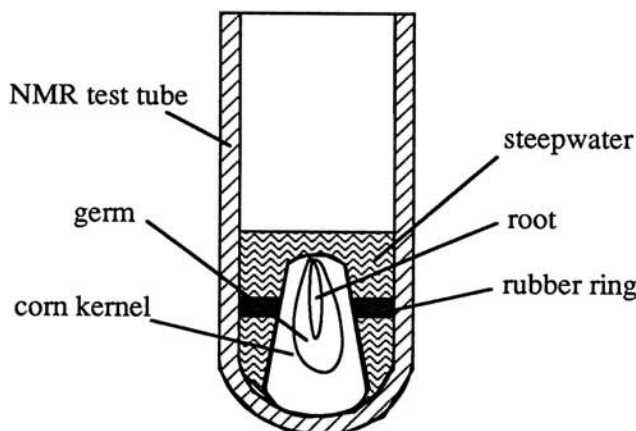


Fig. 1. Schematic diagram of corn kernel during steeping. NMR = nuclear magnetic resonance.

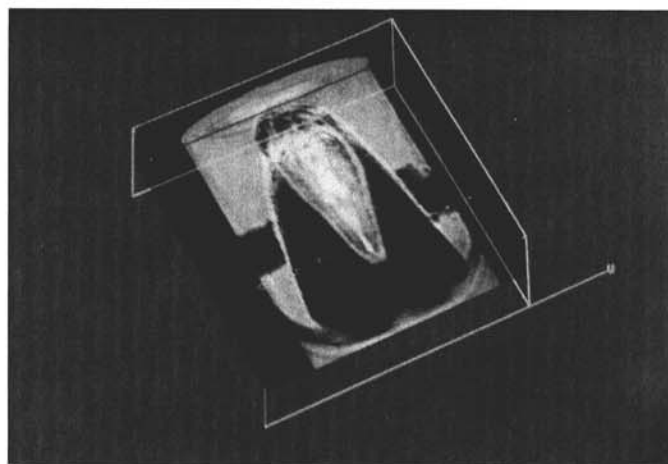


Fig. 2. Three-dimensional image of a corn kernel during steeping (echo delay time = 4.2 msec, repetition delay time = 0.10 sec).

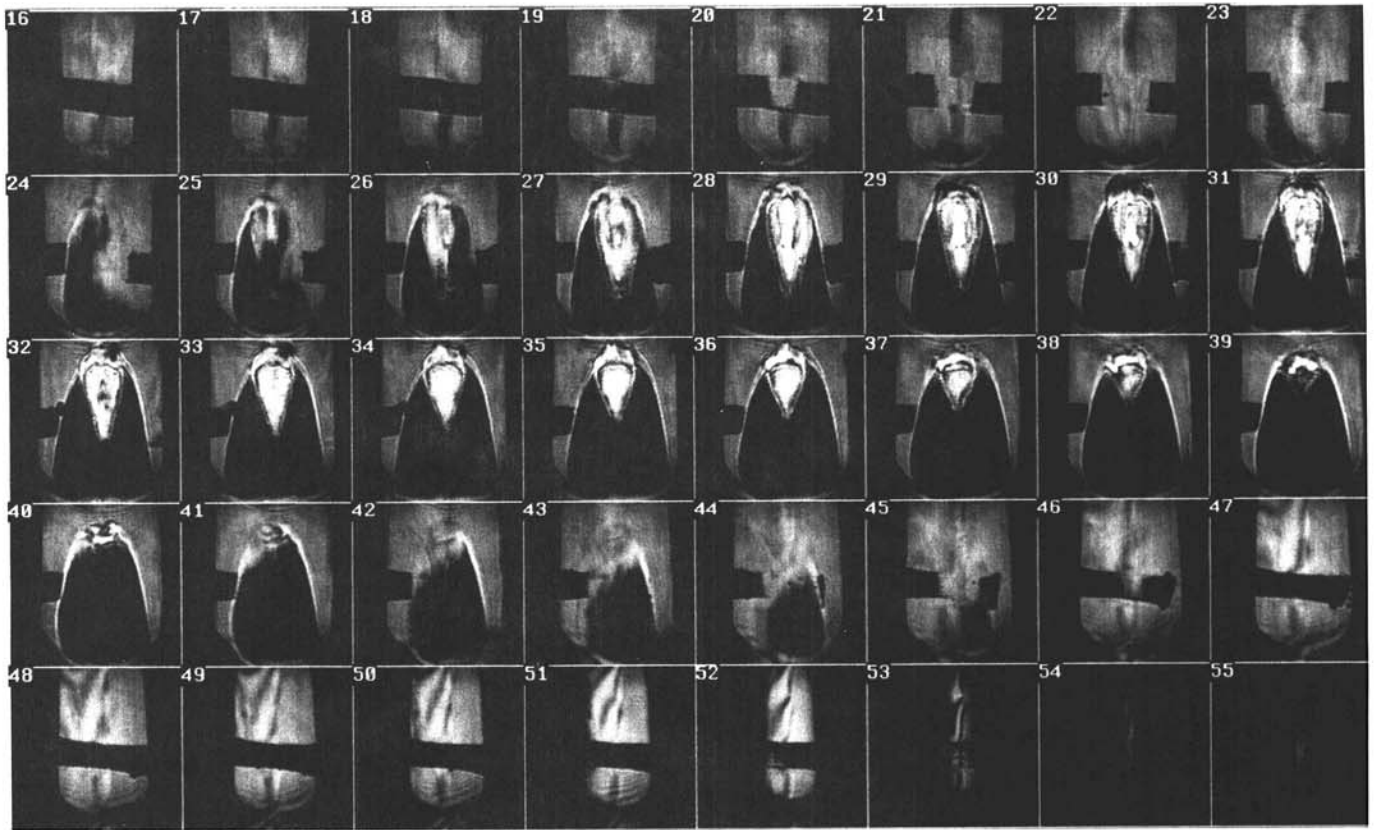


Fig. 3. Forty two-dimensional sequential slices of a three-dimensional image of a corn kernel during steeping (echo delay time = 4.2 msec, repetition delay time = 0.10 sec).

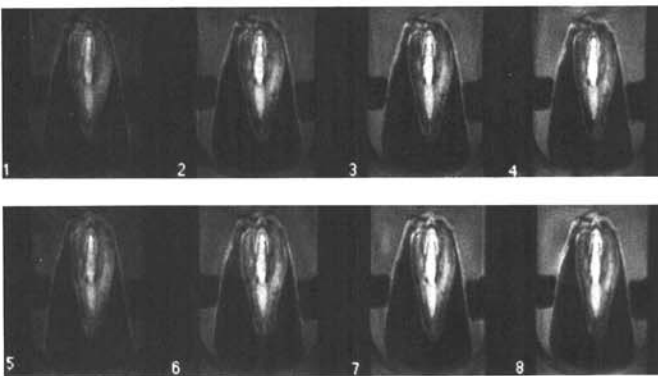


Fig. 4. Two sets of  $T_1$ -weighted images of the same slice of a corn kernel during steeping. Images 1-4 were at 3 hr of steeping and images 5-8 at 6 hr. The echo delay time was 4.2 msec, and the repetition delay times were 0.05, 0.10, 0.15, and 0.20 sec, respectively, for images from left to right.  $T_1$  = spin-lattice relaxation time.

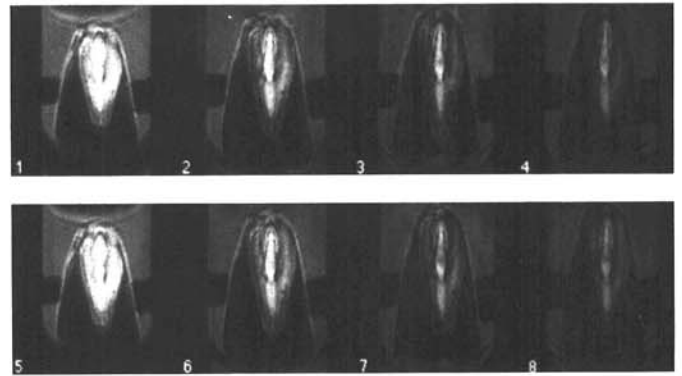


Fig. 5. Two sets of  $T_2^*$ -weighted images of the same slice of a corn kernel during steeping. Images 1-4 were at 3 hr of steeping and images 5-8 at 6 hr. The repetition delay time was 0.10 sec, and the echo delay times were 2.8, 4.2, 5.6, and 7.0 msec, respectively, for the images from left to right.  $T_2^*$  = spin-spin relaxation time.

of the two sets (a total of eight) of  $T_2^*$ -weighted images (Fig. 6). The bright area at the bottom of the tube may be due to magnetic field inhomogeneities because of the lesser amount of surrounding steepwater.

Two  $T_1$  mappings were obtained from the nonlinear fitting of the two sets (a total of eight) of  $T_1$ -weighted images (Fig. 7). Using a regional measurement technique (NIHImage 1989; DataScope 1990), which allows simultaneous displaying of localized image pixels and their actual intensity values,  $T_1$  of the root inside the germ was found to be about 0.3 sec,  $T_1$  of the pericarp about 0.4 sec, and the  $T_1$  of the endosperm about 0.15 sec (Table II). Therefore, the water in the pericarp and the root inside the germ had higher mobility, while the water in the endosperm had the lowest mobility. The proton density of the germ was found to be relatively uniform and high (Fig. 8), whereas that of the

endosperm was not uniform and was low. It was also found that  $T_1$  and  $T_2^*$  did not increase much with steeping time, nor did proton density. The total moisture gain after 8 hr of steeping was about 4% (wb) because the steeping was done at room temperature and with a kernel that had a relatively high initial moisture content. The average values of the  $T_1$ ,  $T_2^*$ , and proton density of some principle components of the corn kernel are shown in Table II.

Also, since the initial moisture content of the corn kernels was high, and the experiments were done at room temperature, the volumetric expansion during each test was very small (less than 1%). The final moisture content of the corn kernels was about 39% (wb). The one-dimensional proton density profiles of the corn kernels (Fig. 9) illustrate that a small increase in proton density took place during the experiment.



Fig. 6. Two  $T_2^*$  images of the same slice of a corn kernel during steeping. The left image was at 3 hr of steeping and the right image at 6 hr.  $T_2^*$  = spin-spin relaxation time.

TABLE II  
Average Values of  $T_1$ ,  $T_2^*$ , and Proton Density of Some Principle Components of the Corn Kernel During Steeping

Component	$T_1$ (sec) <sup>a</sup>	$T_2^*$ (msec) <sup>a</sup>	Proton Density <sup>a</sup>
Germ	0.25	3.0	5.0E06
Root	0.30	4.0	1.0E06
Endosperm	0.10	1.5	2.5E06
Pericarp	0.40	10.0	1.5E04

<sup>a</sup> Mean values from five sample positions.

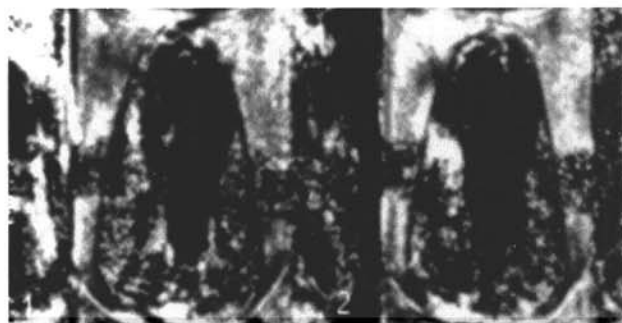


Fig. 7. Two  $T_1$  images of the same slice of a corn kernel during steeping. The left image was at 3 hr of steeping and the right image at 6 hr.  $T_1$  = spin-lattice relaxation time.

As discussed above, the FLASH technique could be used to study the moisture movements inside the corn kernel when there were no large structural changes during each test. The signal intensity from the gradient-refocused sequence increased with an increase of  $T_1$  value and decreased with an increase of  $T_2^*$  value. Therefore, when there are only small changes in  $T_1$  and  $T_2^*$  values, the effect of the increase of the  $T_1$  tends to compensate for the effect of the  $T_2^*$  increase, so that  $T_1$  and  $T_2^*$  factors together might be considered as nearly constant during the experiment. Regular images from the gradient-refocused sequence, or  $T_1$ ,  $T_2^*$ , and proton density weighted image, may be used to examine the moisture changes. For corn kernels with low initial moisture content, and steeped at conventional steepwater temperature (about 50°C), the proton density images are needed to monitor the moisture and movement accurately. This is due to the ineffective compensation between the  $T_1$  and  $T_2^*$  factors caused by the large changes in  $T_1$  and  $T_2^*$  during the tests. Faster imaging sequences would be very helpful in obtaining the  $T_1$  and proton density images, and further work is being done to develop these sequences.

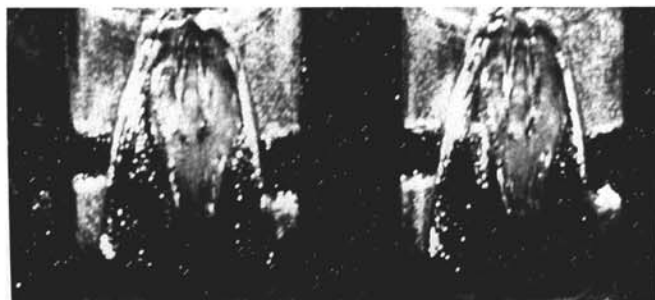


Fig. 8. Two proton density images (calculated proton density mappings) of the same slice of corn kernel during steeping. The left image was at 3 hr of steeping and the right image at 6 hr.

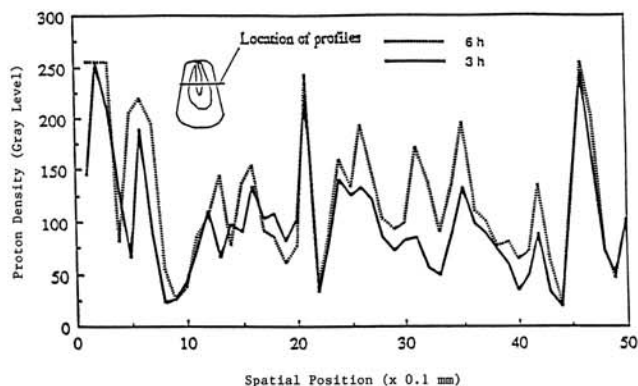


Fig. 9. Proton density profiles at a line across the center of the corn kernel.

## SUMMARY

The gradient-echo fast-imaging technique was modified and explored as a technique to study a corn kernel-steepwater system. The outside steepwater was well suppressed and the inside structure was revealed clearly.  $T_1$ ,  $T_2^*$ , and  $\rho$  mappings were obtained. Water mobility and distribution inside the corn kernel during room temperature steeping was found over the narrow range studied. This technique can be used to study the corn steeping process, such as the  $SO_2$  and lactic acid effects on the structure change and water absorption of maize kernel.

## ACKNOWLEDGMENTS

This study was funded by the National Science Foundation, NSF grant CBT-8808748. Appreciation is expressed to the Biomedical Magnetic Resonance Laboratory at the University of Illinois, P. Lauterbur, Director, for the use of its facilities. Thanks are also extended to C. Potter, National Center for Supercomputing Applications, for providing the image processing software.

## LITERATURE CITED

- CHEN, P., McCARTHY, M. J., and KAUTEN, R. 1989. NMR for internal quality evaluation of fruits and vegetables. *Trans. ASAE* 32:1747-1853.
- DATASCOPE. 1990. Image processing software. National Center for Supercomputing Applications, University of Illinois, Urbana.
- JENNER, C. F., XIA, Y., ECCLES, C. D., and CALLAGHAN, P. T. 1988. Circulation of water within wheat grain revealed by nuclear magnetic resonance microimaging. *Nature* 336:399-402.
- JOHNSON, G. A., BROWN, J., and KRAMER, P. J. 1987. Magnetic resonance microscopy of changes in water content in stems of transpiring plants. *Proc. Natl. Acad. Sci. USA* 84:2752-2755.
- MORRIS, P. G. 1986. *Nuclear Magnetic Resonance Imaging in Medicine and Biology*. Clarendon Press: Oxford, England.
- NIHIMAGE. 1989. Image processing software. National Institutes of Health, Research Services Branch, Bethesda, MD.
- RUAN, R., SCHMIDT, S. J., SCHMIDT, A. R., and LITCHFIELD,

- J. B. 1989. Nondestructive measurement of transient moisture profiles and moisture diffusion coefficient in a potato during drying and absorption by NMR imaging. AICHE Paper 10(d). American Institute of Chemical Engineers, New York.
- SONG, H., and LITCHFIELD, J. B. 1990. Nuclear magnetic resonance imaging of transient three-dimensional moisture distribution in an ear of corn during drying. *Cereal Chem.* 67:580-584.
- STARK, D. D., and BRADLEY, W. G., Jr. 1988. *Magnetic Resonance Imaging*. C. V. Mosby Company, St. Louis.
- VIEWIT. 1990. Image processing software. National Center for Supercomputer Applications and Biomedical Magnetic Resonance Laboratory, University of Illinois, Urbana.
- WEHRLI, F. W., MacFALL, J., and NEWTON, T. H. 1983. Parameters determining the appearance of NMR images. Pages 81-117 in: *Advanced Imaging Techniques*, Vol. 2. T. H. Newton and D. G. Potts. eds. Clavadel Press, San Francisco.

[Received January 24, 1991. Accepted July 1, 1991.]